

LASER SHEAROGRAPHY- PREDICTION AND OPTIMIZING ITS FLAW DETECTION CAPABILITIES USING AN ADVANCED HYBRID APPROACH

Y. Elbaz and H. Abramovich

Faculty of Aerospace Engineering Technion, I.I.T., 32000 Haifa, Israel

Abstract

In recent years, there is significant integration of composite materials in the aircraft structure due to their unique benefits. Flaws in composite structures may be formed already during the manufacturing process or during service. These flaws may develop in different areas of the aircraft and cause structure failure and even a flight safety incident. Effective and reliable NDT (non-destructive testing) capability is the guarantee for early structural flaws detection to maintain the integrity of the aircraft structure and ensure flight safety.

One of the main NDT methods, which has been gaining momentum in recent years, is the Laser Shearography Testing (LST). It is based on the analysis of the optical derivative of the perpendicular displacement of the surface being examined under excitation. This method uses laser and interferometric imaging, which can be used to detect subsurface flaws.

Today, due to dependence on several parameters, the detection capabilities of the LST, are not known in advance and individual experiments using dedicated test specimens are required - each case on its own. Therefore, the application of the LST method the NDT procedures is based on accumulated experience, trial and error, and a number of "rules of thumb" yielding only a general assessment, if any, of the manner in which the flaws are modulated and stimulated.

In the present study, a theoretical, analytical, and experimental study of the engineering prediction of Shearography fringe pattern is presented. Based on mathematical and the physical models of the LST, a methodology was developed and implemented as a simulation to evaluate the LST fringe pattern in advance. This simulation focuses on a circular delamination flaw that is stimulated by vacuum excitation. The simulation was verified by comparing its results to representative cases from the literature and by conducting a practical experiment using a LST system. The simulation results showed a good agreement with the experimental ones. Subsequently, "Detection Capability Envelopes" were constructed for the LST method enabling the assessment the flaws detection capability in advance, depending on a variety of parameters. Investigation of the detection capability and construction of these envelopes was applied for the three most common types of skin structures in aviation – aluminum, composite solid laminate, and composite sandwich.

This methodology and technique will allow a more correct and accurate design of the test specimens and lead to optimal test parameters defining process by a hybrid approach. In addition, the hybrid method can be used as a guide and as a reference point for all those involved in the testing process using the LST method, developers, and technicians alike, for the more efficient and accurate flaws detection in aviation structures – which will lead to improvements of the flight safety.

Keywords: LST, shearography. NDT. Composite materials, flaws

Introduction

In recent years, the aviation world has experienced major changes in the field of aircraft structure. One of the important ones is the significant integration of elements made of composite materials due to their unique benefits [1]-[4]. Today, these materials are integrated both as secondary structural parts, as has been done for many years, and as primary structural

parts, carrying a significant load on the aircraft [5]-[7]. This trend is expected to intensify in the coming years [8].

Despite their well-known structural advantages, like superior strength to weight ratio, composite materials show a sensitivity of the final product to the various manufacturing processes [9] and some limitations for the application of various non-destructive testing – NDT Methods. Flaws in composite materials may be formed either during the manufacturing process or in the course of the normal service life of the component [10]. While it can be assumed that strict quality assurance will lead to a reduction in manufacturing flaws, service flaws may arise due to poor design, a change in the operating spectrum (fatigue) or an external impact [11].

Unfortunately, the flaw detection is a challenging task because the flaws are hidden in between the layers and are invisible [12]. Testing of composites structures is a global challenge due to the faster progress of production capabilities in relation to testing ability, as has happened in the past in the world of metals.

In a composite structure, there is an inherent variability of its medium. This variability is manifested both at the level of the individual layer (micro), which is made of fiber and matrix and has a fiber arrangement in varying directions, and at the macro level - there are different structural elements (layers, cores, etc.). This medium variability constitutes a challenge in transferring excitation energy (thermal, mechanical, acoustic, electrical, etc.) to the structure medium and its absorption back in a satisfactory SNR (Signal to Noise Ratio), to analyse the integrity of the structure.

There are various factors that affect the NDT of a composite structure: layers thickness, plies orientation, arranging the elements, etc. In addition, composite structures may contain elements that scatter or absorb the excitation energy, which is used to detect the flaws. These elements (such as Rohacell foam and honeycomb core) limit the ability to penetrate to the depth of the medium being tested and reduce the ability to detect flaws.

To provide adequate solutions for the challenges imposed by composite materials a number of non-destructive techniques has been proposed. There are five major non-destruction methods for testing composite structures: Tapping, Ultrasonic (UT), Shearography (LST), Thermography (IRT) and Acoustic emission (AE) and their derivatives. These methods use an energy source (thermal, acoustic, mechanical) to inject the energy into the structure medium and absorb its reflection on the surface in a high SNR and thus detect flaws in the depth of the medium. This principle meets the challenges of the composite materials, which constitute a variable medium that is not continuous and sometimes has elements that dissipate or absorb energy and therefore make it difficult to detect flaws in the depth of the tested medium (see [13] for a detailed description of the methods).

Among the various new NDT techniques, optical ones are emerging as strong tools, because of their nature of being full-field, non-contacting, and non-contaminating. Moreover, the results of the inspection of optical methods are images that give visual representations of the components condition [14].

One of these methods is Laser Shearography Testing (LST - also called Speckle Pattern Shearing Interferometry - SPSI) was first introduced as a full-field strain analysis technique by Hung and Taylor [14].

The principles of the LST method are based on physical principles (electromagnetic waves, light and matter interaction, wave interference, laser, interferometry etc.) which were introduced many years ago but due to technological limitations, system development which will be a practical solution has been delayed until the recent years.

LST is an NDT technology based on the optical derivative analysis of the displacement perpendicular to the surface being examined under excitation. This method uses laser and interferometric imaging, which can be used to detect subsurface flaws in the depth of the medium [15]-[18]. This method offers optimal conditions for direct measurement of strain information in the test specimen. As flaws usually generate strain concentration, LST reveals a flaw within the tested part by identifying flaw-induced strain anomalies. Flaws in the part will

give rise to strain concentrations when the part is loaded, and the strain concentrations form a fringe pattern that is used to detect and analyse the flaws [14]. LST applies laser light to the surface of the tested part while the part at rest (non-stressed) and the resulting image is picked up by a charge-coupled device (CCD) and stored on a computer.

Then the surface is stressed, and a new image is generated, recorded, and stored. The computer then superimposes the two patterns and if flaw such as voids or disbonds is present, the flaw can be revealed by the developed patterns. Discontinuities and flaws as small as a few micrometers in size can be detected using this approach.

Unlike other methods of speckle interferometry, e.g., ESPI (Electronic Speckle Pattern Interferometry), the interference in LST is generated by two identical, laterally sheared object beams. This effect can be realized by a shear element which is located between the object and camera. Since no additional reference beam is needed, the setup for LST is simple and with no need of vibration isolation compared to other coherent optical techniques. Thus, compared with ESPI, LST is relatively insensitive to disturbances from the environment and is a robust method to be applicable in industrial environments.

LST has a high sensitivity to local deformation over the surface of the tested part. This deformation is due to internal and / or external discontinuity in the subject being excited. In practice, using the LST system, very small perpendicular deformations (Z axis) can be detected: 2-20 nm, but there is a dependence on the environmental conditions that might affect the test results.

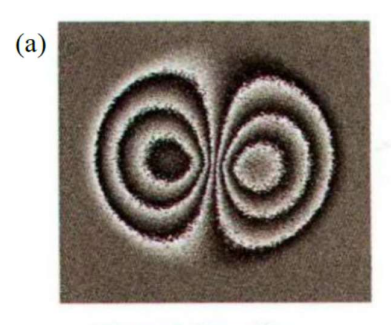
The derivative of the surface route is the optical shear of the laser speckle pattern. This shear is performed by a cube beam splitter in a Michelson interferometer. Controlling the size and direction of the shear vector (by moving the interferometer mirrors) provides the ability to reduce the relative displacement effect between the test system and the test structure and adjust the directional and general sensitivity of the test. These allow to perform an optimization for identification of minor changes on the tested surface and at the same time reduce the effects that might interfere with the performance of the test.

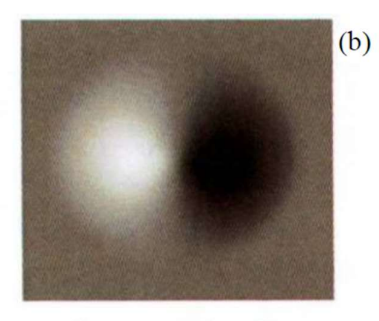
Common excitation methods in LST are heating, pressure, and vibration (mainly acoustic, using ultrasonic vibrators or transducers). Choosing an appropriate excitation technique is critical to the success of the test. Appropriate excitation (e.g., heating of a surface in a metal Honeycomb structure), will result in a different displacement of the surface in normal area (without discontinuities) relative to the surface above the discontinuity. Optical shear of the surface will lead to a more accurate detection of the discontinuity from a top view (C-Scan display).

Thus, although the laser beam does not penetrate below the tested surface, the LST method can be used to detect discontinuities such as: impact damage, non-adhesion, delaminations, inclusions, porosity near the surface, wrinkles, fiber-bridging, cracks, etc.

The result of LST is named a "shearogram". The shearogram is created by processing of the interference pattern derivative of the tested surface in both strain states of the surface being tested - before and after the excitation (sometimes even during it). Due to the use of the optical derivative of the test surface, a typical indication form of discontinuity, as obtained by LST, is a "double lobe" (see Fig. 1a). In this way, the shearogram is a phase change map, which represents at each point the phase change of the laser beam (which returns from the surface being tested and is captured by the camera detector). These phase changes are created by the vertical displacement difference of the surface being tested - before and after excitation. There are two to ways to display the shearogram:

- Wrapped phase map display where fringes can be seen, when each fringe represents an equal-strain line.
- Unwrapped phase map display is the product of an integration process of all the fringes in a certain direction (defined by the shear vector), where each fringe represents a phase cycle from 0 to 2π . Thus, a normalized image is obtained which is a general average of the derivative white (positive derivative), black (negative derivative), as shown in Fig 1b.





Wrapped Phase Map

Unwrapped Phase Map



Fig. 1- Shearogram displays: (a) Wrapped phase map, (b) Unwrapped phase map (adapted from [20])

A detailed review on LST method can be found in [13] including the pros and cons of the approach.

The present study, focuses on the application of the LST method by mechanical excitation - with emphasis on vacuum excitation. In this case, the resulting shearogram represents the map of the phase changes of the laser waves between the following two modes: before excitation (without suction for pressure change) and after excitation (activation of suction and pressure differentiation).

Through the efforts of worldwide scholars, LST has been successfully applied to NDT of a variety of structures. However, due to the LST dependence on the test system optics and on the structure and flaw properties – there is a challenge to assess the detection capabilities of the LST method in advance (before preforming the test). In addition, during the detection process, the loading methods and system parameters depend largely on the experience of the operator, which affect the effectiveness and accuracy of the test.

Therefore, LST is a comparative non-destruction test that requires the use of dedicated test specimens (). These specimens are sometimes (especially for composite structures) very expensive, complex to manufacture and there is difficulty in simulating within them the flaws required for detection.

To evaluate the LST detection capability ahead of time (without performing a series of tests based on trial and error using test specimens), increase the test accuracy and make it easier to select the optimal parameters - in this study we built a hybrid engineering model that allows us to evaluate the LST detection capability.

This model is based on the LST fundamental equation, namely, if the vertical displacement derivative of the test surface can be estimated (by closed solution or FEA), then the abstract fringes pattern can be predicted. The engineering model was coded as a simulation. This simulation was tested by comparing its results to representative cases from the literature and by conducting a practical experiment by LST system.

Subsequently, "Detection Capability Envelopes" (DCE) were constructed for the LST method and make it possible to assess the detection capability of flaws depending on a variety of parameters: the material of the structure (E, v), flaw depth (h), flaw size (a), loading intensity $(P - pressure or concentrated force), wavelength <math>(\lambda)$ and shearing amount (Δs) .

These envelopes exist only partially (if at all) and for specific cases only. The simulation developed in the present study as well as the detailed DCE will make it possible to know the detection capability of the LST method in advance and will save unnecessary production of test specimens.

Methodology

As stated above, the present study, focuses on the application of the LST method by vacuum excitation. Using this technique, for a particular test system, it is not possible today to predict apriori the shearogram in a convenient and immediate way. This drawback will be eliminated by the present study.

Flaw detection capability, which is analyzed from the shearogram, directly dependent on the size and the manner of the surface displacement (w(x,y,z)) above the flaw under vacuum excitation P(x,y). The present study focuses on a circular delamination flaw as schematically presented in Fig.2.

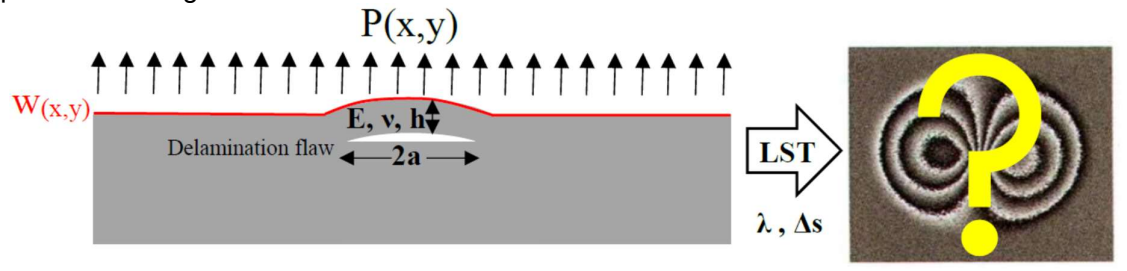


Fig. 2- A circular delamination flaw-the various factors affecting the output shearogram

The shearogram prediction challenge stems from the fact that the change in the surface contour function w(x,y,z) (in the perpendicular direction) under vacuum excitation P(x,y), depends on a number of factors affecting the structure response: excitation properties (distribution and intensity), structure properties, flaw properties and on the properties of the piece of structure above the flaw. Also, the characteristics of the test system (shear vector and laser wavelength) have an effect on the ability to detect and display the flaw indication.

To analyze the perpendicular displacement of the surface above a circular delamination flaw, the basic structure model is an isotropic circular plate having a radius \mathbf{a} and loaded by a uniform pressure \mathbf{P}_0 (see Fig.3). The boundary conditions is a fully clamped one, for which there is an analytical deflection solution [21] as a function of the distance \mathbf{r} from the center of the plate (see Eq. 1).

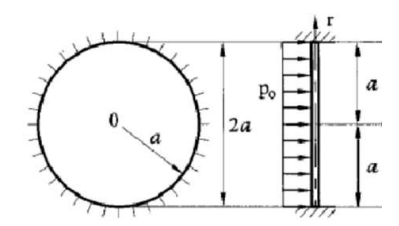


Fig. 3 - An all around clamped circular plate, under normal pressure (adapted from [21])

The vertical deflection of an all around clamped circular plate is given by [21],

$$w(r) = \frac{p_0}{64D} (a^2 - r^2)^2$$
 where
$$D = \frac{Eh^3}{12(1-v^2)}$$
 (1)

and w(r) is a perpendicular deflection, p_0 =vacuum excitation intensity (pressure), D stands for the bending stiffness, h is the plate thickness, while E and u are the Young's modulus and the Poisson's ratio, respectively.

Note that for other types of loading, like a concentrated force (F) at the center of a clamped circular plate (namely a force constraint) we have [21]

$$w(r) = \frac{F}{16\pi D} \left[a^2 - r^2 + 2r^2 \log \frac{r}{a} \right]$$
 (2)

or for a displacement constraint [22]

$$w(r) = \frac{2w_{max}}{a^2} \left[r^2 \log \frac{r}{a} + \frac{1}{2} (a^2 - r^2) \right]$$
 (3)

Equations 1-3 provide satisfactory solutions and can be used to obtain estimated solutions also for plates made of composite materials [23].

Note that the deflection for a circular orthotropic plate can be somehow complicated as the mechanical properties of the composite material is given in Cartesian coordinates, while the circular plate uses cylindrical coordinates. Therefore, the equivalent bending stiffnesses D_{eq} for orthotropic laminated plate were calculated using a MATLAB dedicated code. The code predictions were successfully validated with results from the literature. To increase the reliability of the output, FEM models were used and implemented in the MATLAB code. The LST results are obtained using the block diagram presented in Fig. 4.

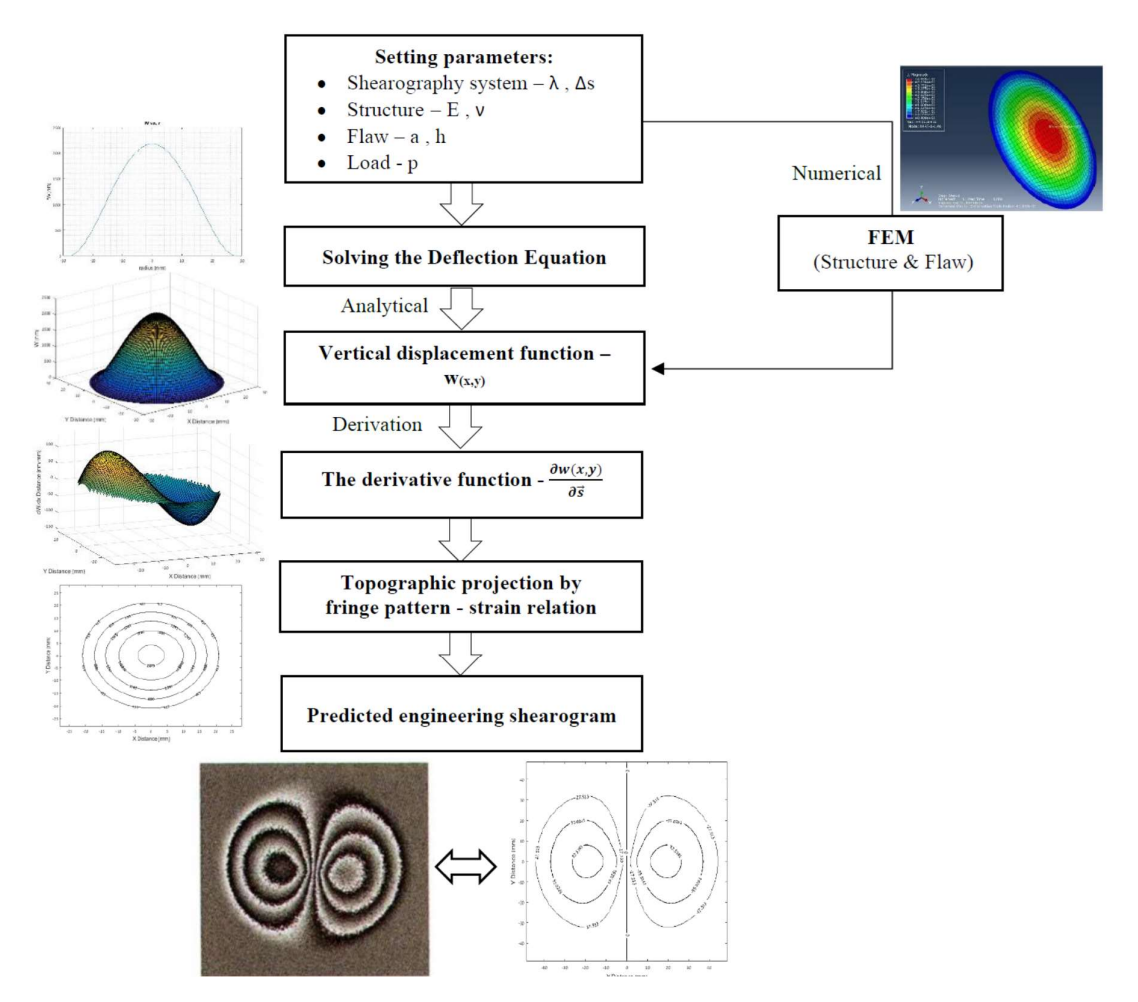


Fig. 4- Block diagram for the methodology implementation of the prediction simulation

The present LST prediction simulations were first compared with existing results presented in the literature. Typical results are presented in Figs. 5 and 6. More results are given in [13].

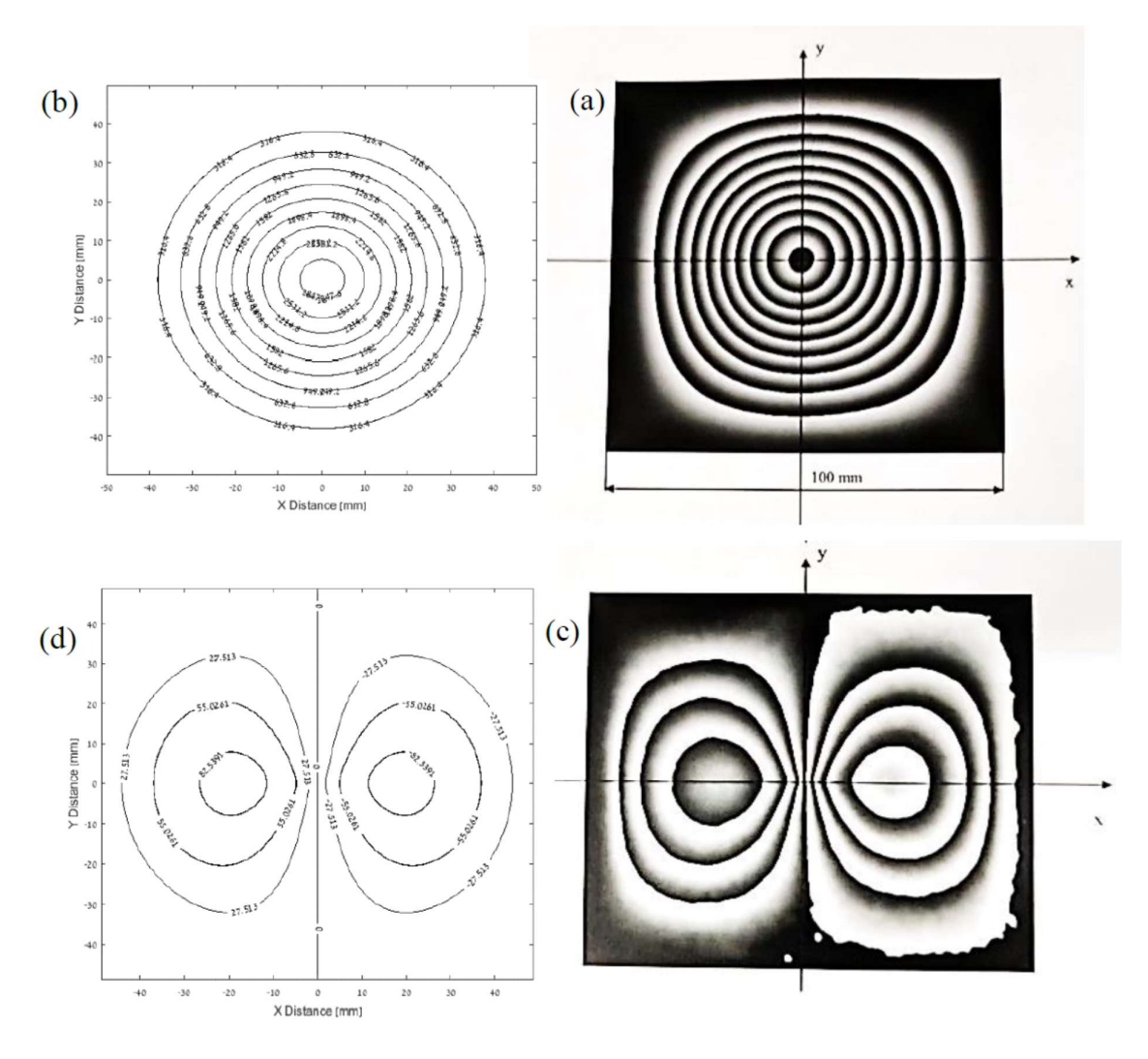


Fig. 5 - Literature test cases-(a) Experimental hologram obtained in [24], (b) Hologram obtained by the present simulation, (c) Experimental shearogram presented in [24], (d) Shearogram obtained by the present simulation.

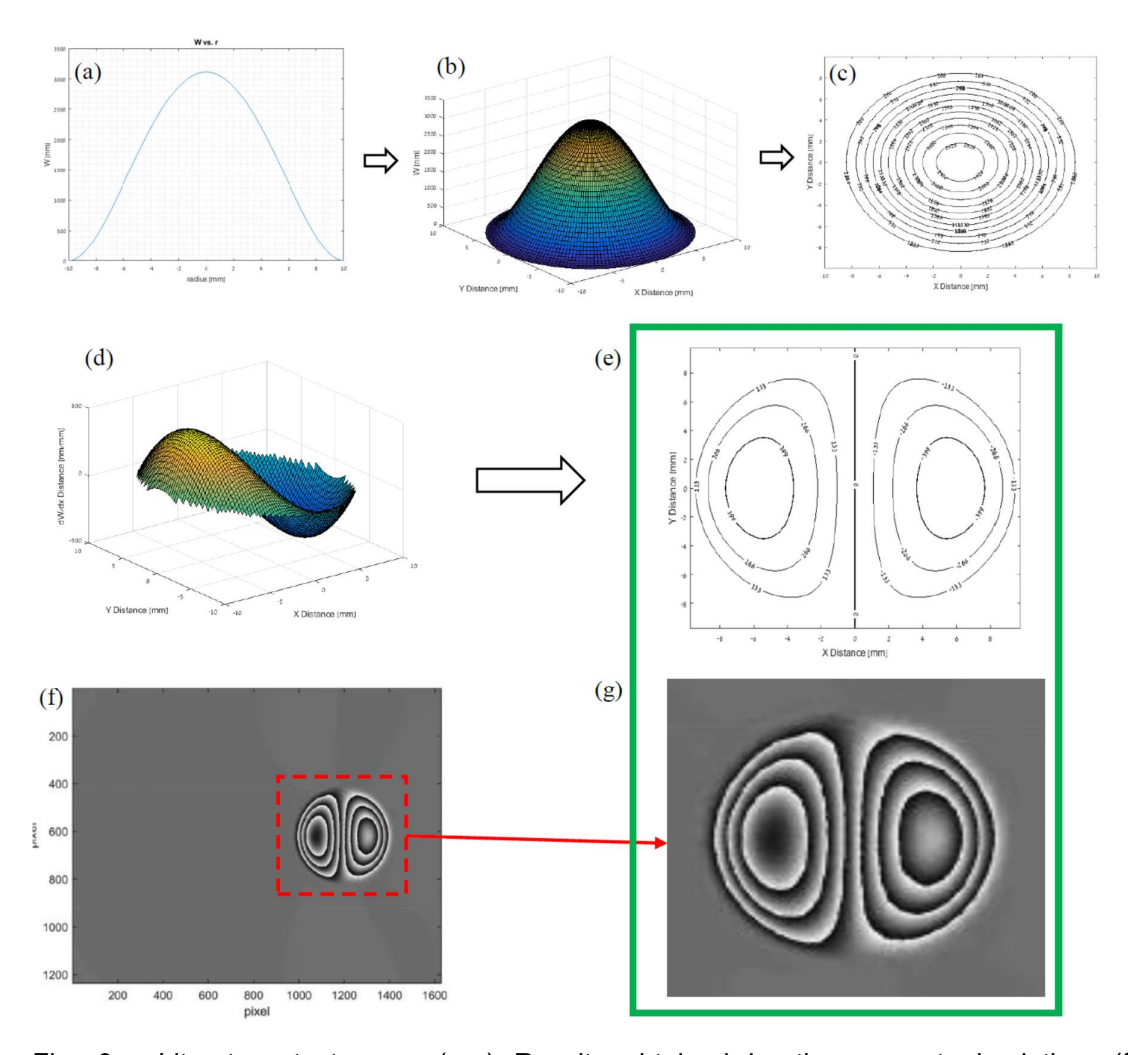


Fig. 6 - Literature test cases-(a-e) Results obtained by the present simulation, (f-g) Experimental shearogram presented in [25].

As can be observed from Figs. 5 and 6, there is an excellent matching between the present simulation results and the experimental results from the literature.

Test set-up, specimens and results

The simulation shearogram predicted results are compared with experimental results, using the LTI-5200HD mobile system, presented in Fig.7.

The first specimen was a aluminum 6061-T6 plate (see Fig.8a) having a centred flat bottom hole, FBH, to simulate a delamination flaw (diameter -2.5 inches=63.5 mm, depth 1.5mm).

The second specimen (Fig. 8b) is a composite one containing 21 flaws, some circular and some square, some of which are simulated by FBH and some are simulated by implanting Teflon sheet. The presents study focuses on flaws 17, 19 and 21 which simulates circular FBH delamination (diameter- 1 inch=25.4 mm, depth 1mm).

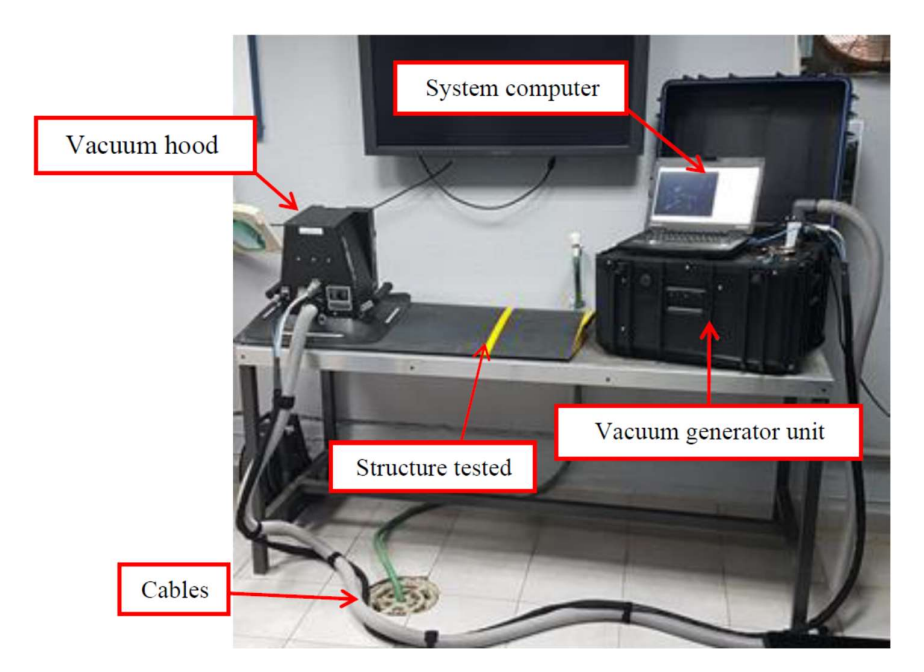


Fig. 7-The LST test system- LTI 5200HD

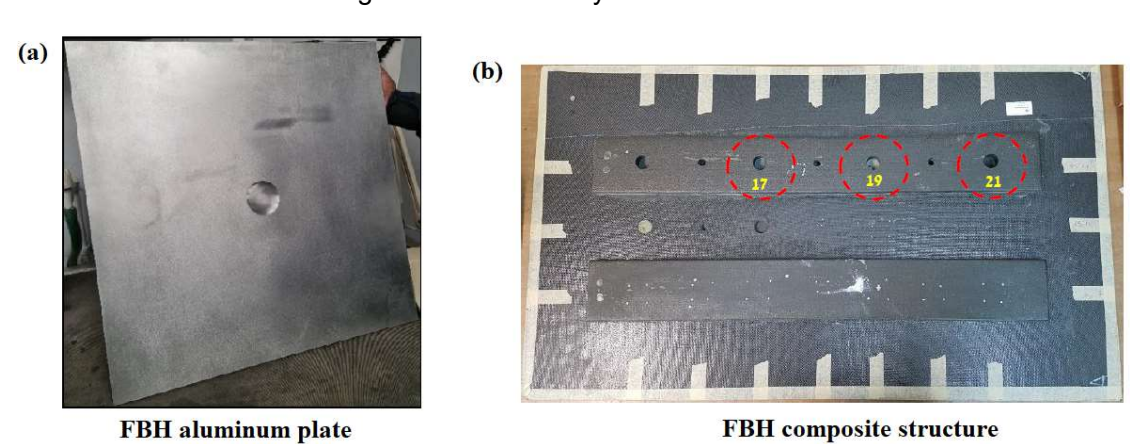


Fig. 8-Test specimens-(a) FBH aluminum plate, (b) FBH composite structure

The experimental results for the aluminum specimen are presented in Fig. 9. Some comments of the picture presented in Fig. 9.

- In contrast to the simulation in which "closed" fringes were obtained, it can be seen that "open" fringes were obtained in the actual experiment. This is due to the effect of the 3 legs of the vacuum hood (two up and one down) which create local pressure. This pressure creates a strain field which affects the strains field that the flaw creates under its excitation.
- It can be seen that the indication of a delamination flaw in the above shearogram is obtained in its characteristic form a double lobe (bounded in the illustration above by the yellow border).
- In the above shearogram, it can be seen that the area where there is a laser stain, which is formed due to the laser returning to the camera from the tested surface, does not contain a phase information (fringes).

 The middle fringe belongs to one of the lobes due to a slightly asymmetrical displacement. We will refer to this fringe as the "symmetry fringe" between the two lobes.

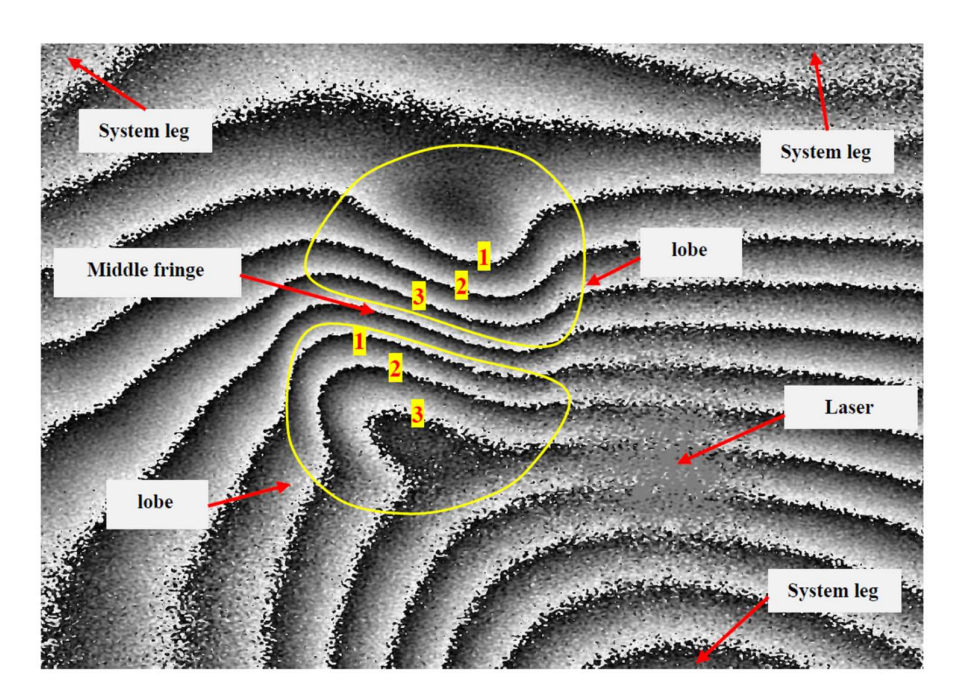


Fig. 9 - Aluminum test specimen- 3 fringes shearogram

Table 1 presents the pressure excitation intensities and the FN (Fringes Number) results obtained in the series of performed experiments.

Table 1. Aluminum test specimen – experimental results

Structure type Test No.	P _i [inchH ₂ O]	P _f [inchH ₂ O]	$\Delta P = P_f - P_i$ [inchH ₂ O]	$\Delta P = P_f - P_i$ [Pa]	FN (for one lobe)
1	24	28	4	996.36	1
2	24	31	7	1,743.63	2
3	24	33.5	9.5	2,366.355	3
4	24	36	12	2,989.08	4
5	24	38.5	14.5	3,611.805	5
6	24	41	17	4,234.53	6
7	24	44	20	4,981.8	7
8	24	46.5	22.5	5,604.525	8
9	24	49.5	25.5	6,351.795	9
10	24	52	28	6,974.52	10

Figure 10 presents the shearograms (wrapped phase map) for the 10 experiments performed on the aluminum specimen.

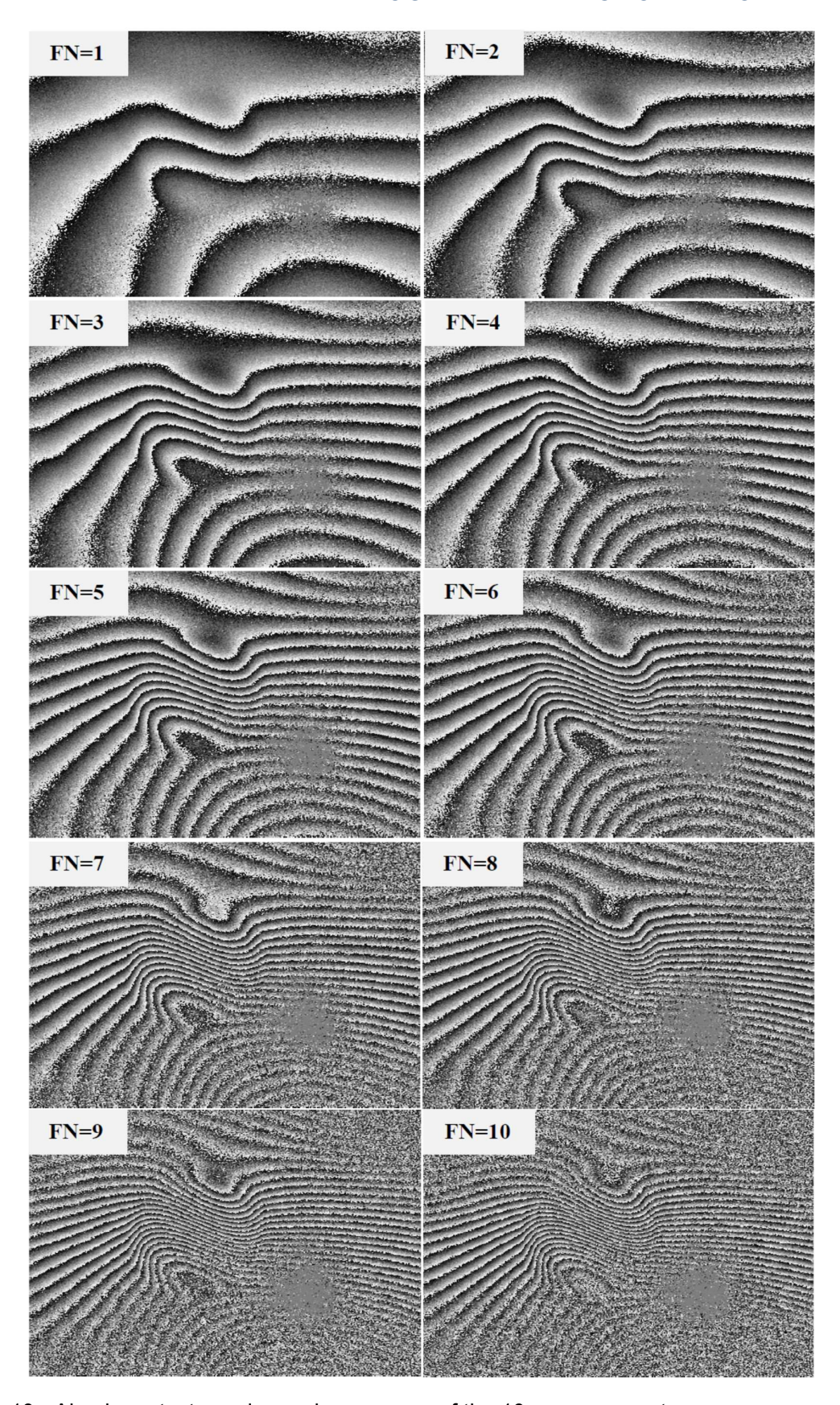


Fig. 10 - Aluminum test specimen-shearograms of the 10 measurements

Note, that for higher pressure excitation intensities, the FN will increase until the fringes reach an undistinguishable state. Moreover, at this state, a transition to unwrapped display creates a decorrelation due to too much vertical displacements for processing.

A comparison was performed between the test results and the output of the present simulation, yielding a good match between the two (see Fig.11).

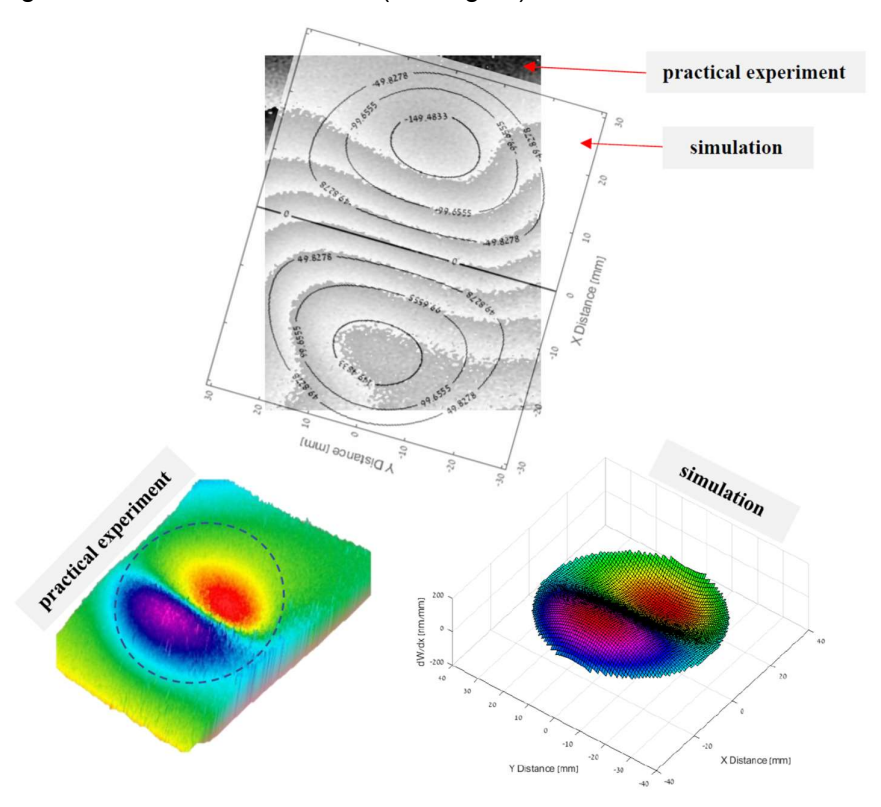


Fig. 11 - Aluminum test specimen- shearogram and 3D vertical displacement derivatives between test results and the present output simulation.

Next a solid composite laminate was tested having a flaw (flaw # 21 in Fig. 8b). The test results are presented in Figs. 12,13 and Table 2.

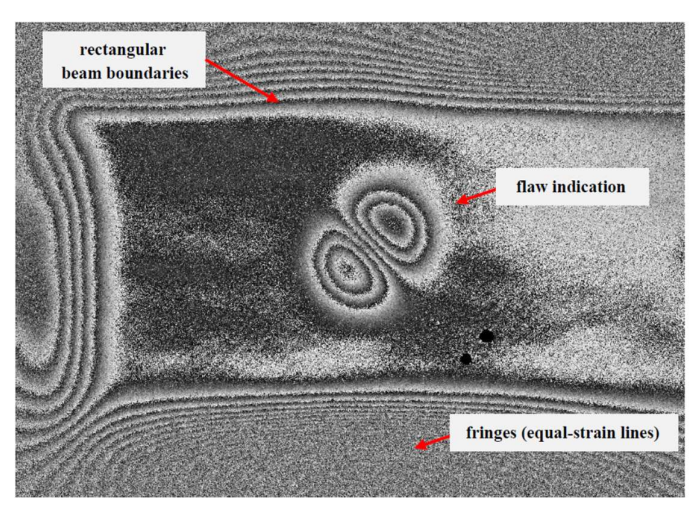


Fig. 12 - Solid laminate test specimen- experimental wrapped display

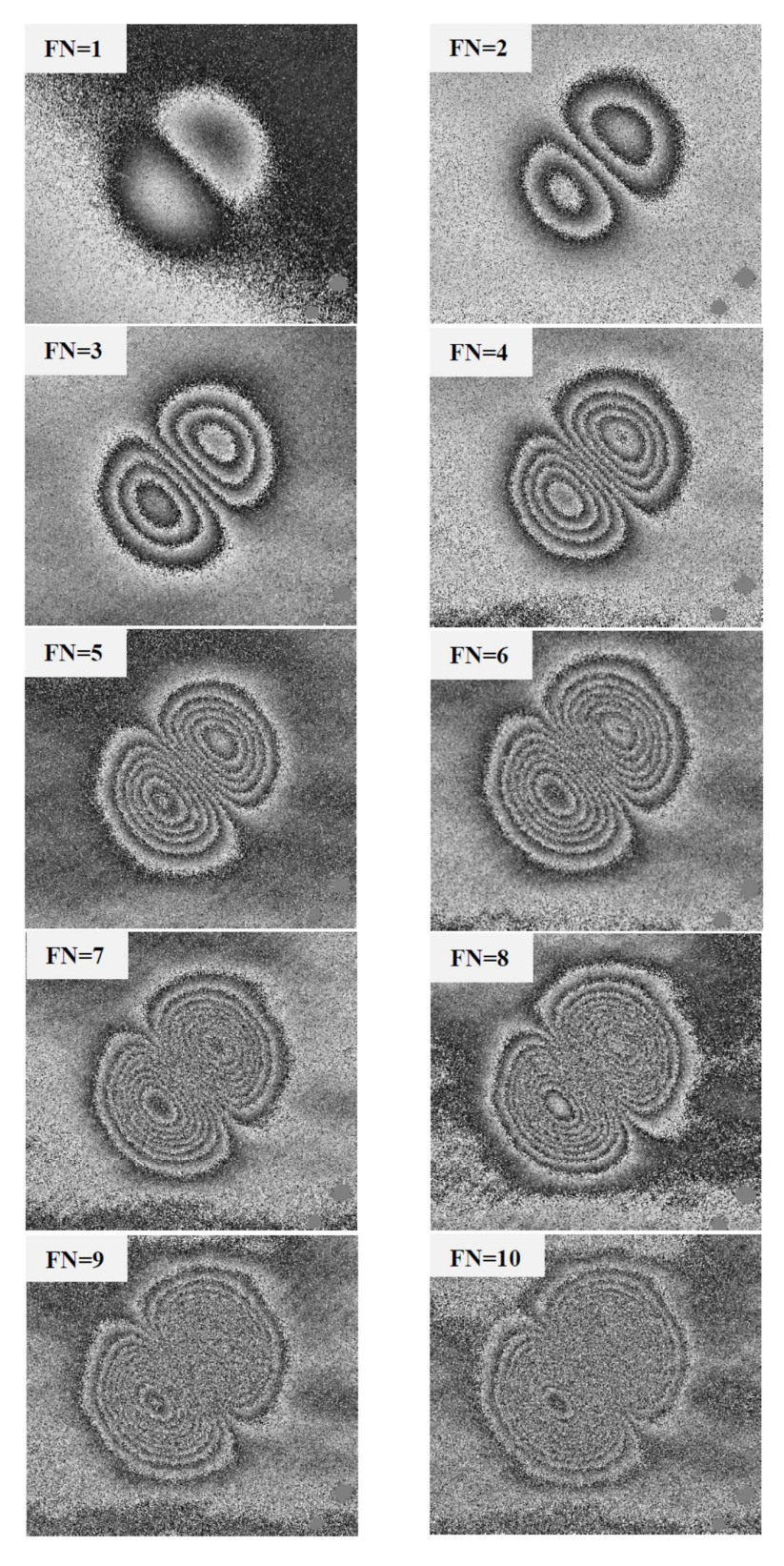


Fig. 13 -Solid laminate test specimen -shearograms (wrapped phase map) of the 10 performed measurements

Table 2 Solid laminate test specimen – experimental results

Structure type Test No.	P _i [inchH ₂ O]	P _f [inchH ₂ O]	$\Delta P = P_f - P_i$ [inchH ₂ O]	$\Delta P=P_f - P_i$ [Pa]	FN (for one lobe)
1	25	29	4	996.36	1
2	25	34	9	2,241.81	2
3	25	39	14	3,487.26	3
4	25	44.5	19.5	4,857.255	4
5	25	50	25	6,227.25	5
6	25	55	30	7,472.7	6
7	25	60	35	8,718.15	7
8	25	65	40	9,963.6	8
9	25	70	45	11,209.05	9
10	25	75	50	12,454.5	10

A comparison was then performed between the practical experiment performed on the solid laminate and the present dedicated simulation, while considering the equivalent bending stiffness approach. To ilustrate the good match between the results, the cases where FN=3,4,5 (in each lobe) are next displayed in Fig. 14.

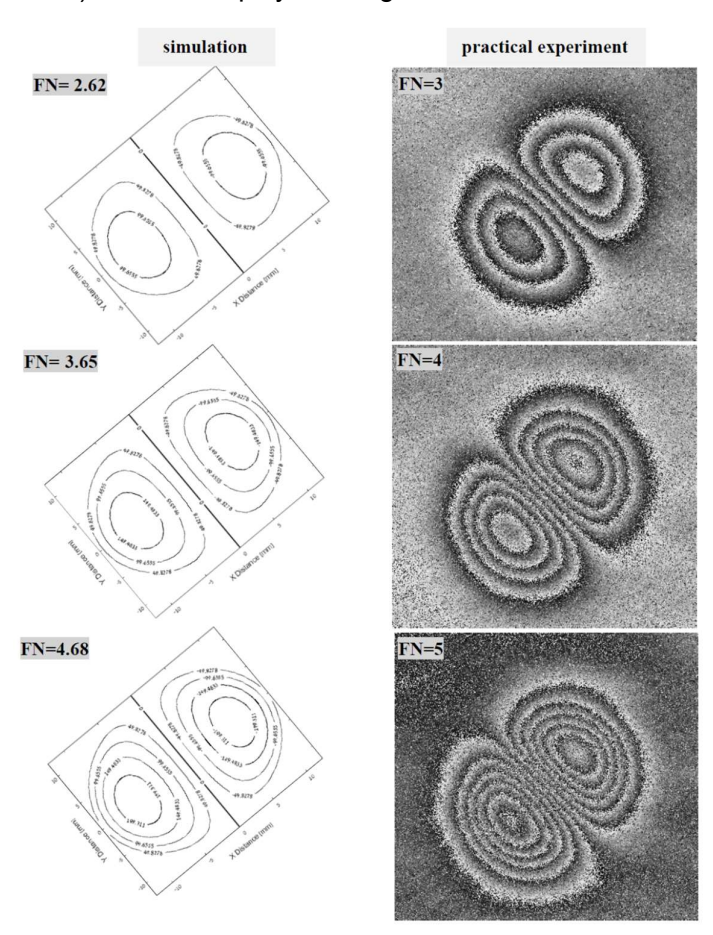


Fig. 14- Solid laminate test specimen-shearogram results comparison

As can be observed from Fig. 14, a good match was obtained between the experimental results and the simulation ones. It is important to notice that the FN predicted by the simulation was about 0.4 lower than the FN obtained in the experiments, however one must remember that partial fringes cannot be predicted by the present dedicated simulation.

Tests were performed also on FBH composite sandwich structure, leading to good matching between the experimental and simulation predicted results. Due to lack of space in the present manuscript, the readers are referred to Ref. [13] which describes in detail the outcome of the composite sandwich structure results.

Detection capability envelopes-typical results

Based on the results and the investigation performed within the present study, some relationships between the FN (fringes number) and the geometry of the flaw (diameter and depth) had been derived and calculated for a given specimen made of aluminum (2024-T3), with a prescribed vacuum pressure excitation intensity, ΔP , shear size Δ and wavelength λ (see [13]). The relationship between FN and the flaw radius, a, can be written as :

$$FN = C[E, \nu, h, \Delta P, \lambda, \Delta s] * [2a]^2$$
(4)

while the relationship between the FN and the depth of the flaw, for a given flaw diameter 2a is

$$FN = C1[E, \nu, \alpha, \Delta P, \lambda, \Delta s] * [h]^{-3}$$
(5)

C and C1 are constants to be approximated for a given data. For example, for an aluminum specimen, E=73.1 GPa, υ =0.33, h= 2mm, Δ P=20 (inch H₂O], λ =830 [nm] and Δ s=12.7 [nm] Eq. [4] turns to

$$FN = 8.0 * 10^{-6} * [2a]^2 \tag{6}$$

while Eq. 5 would be (using the same data as above, and a=1 inch)

$$FN = 8.8898 * [h]^{-3} \tag{7}$$

Using the prediction simulation, not only the effect of each parameter on the detection capability (FN) can be analysed individually, but it is also possible to create detection capability envelopes (DCE) and analyse the effect of several parameters simultaneously. A typical result is displayed in Fig. 15. Based on the result presented in Fig. 15, the DCE is constructed by dropping contours of the FN function onto the X-Y plane (see Fig.16), where each contour indicates the fringes number which is expected to be obtained in a practical LST test.

DCE were constructed for solid laminate and sandwich structure. More details and examples can be found in [13].

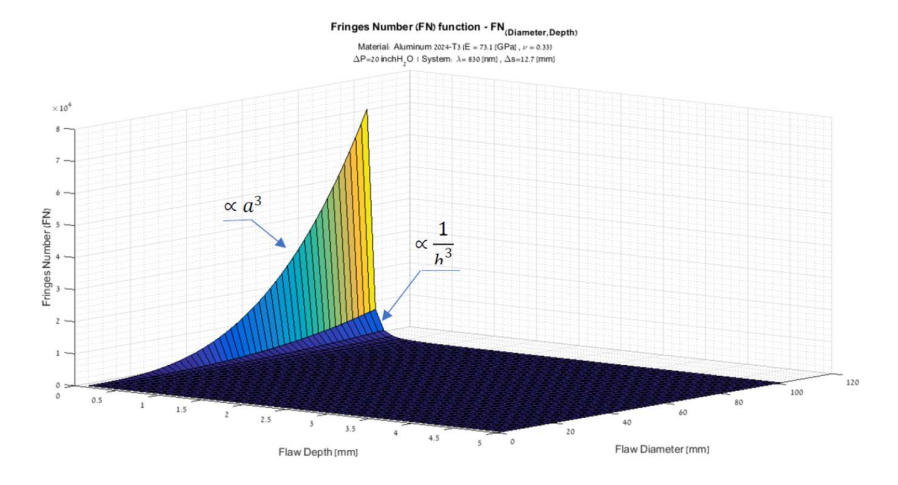


Fig. 15- Aluminum 2024-T3- FN vs. Flaw depth and diameter { $\Delta P=20$ (inch H₂O], $\lambda=830$ [nm] and $\Delta s=12.7$ [nm]}

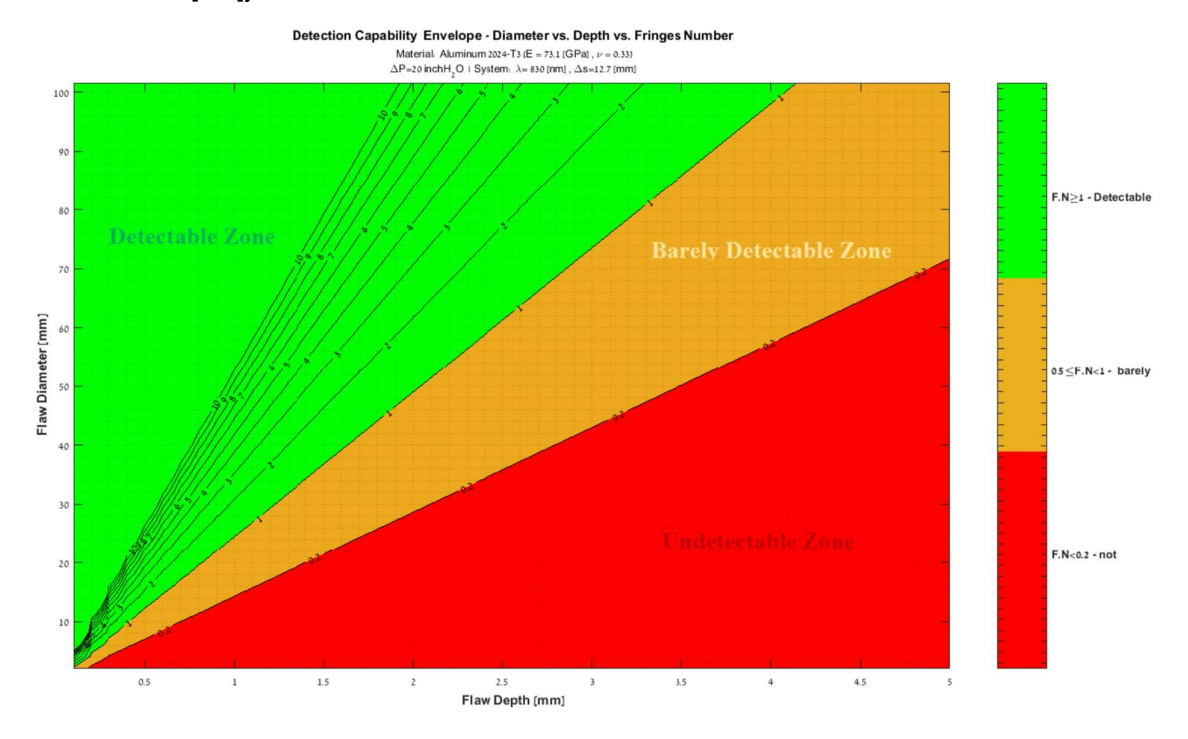


Fig. 16 - Aluminum 2024-T3- Detection capability envelope { $\Delta P{=}20$ (inch $H_2O], \,\lambda{=}830$ [nm] and $\Delta s{=}12.7$ [nm]}

Summary and conclusions

The present study presents a theoretical, analytical and experimental study of the engineering shearography fringe pattern prediction. First, the challenges that exist today in non-destructive testing of composite structures are outlined. Then, the LST method as providing a specific response to these challenges and its mathematical and physical models is introduced. In addition, a comprehensive research literature review on the LST method and the main research activities performed in its field in the past and in the recent years was conducted.

From the challenge of detecting flaws in composite structures by non-destructive manner, our engineering experience and the research review – it emerged that the flaw detection capability

by LST depends on a variety of factors: test system, excitation technique, load intensity, structure and flaw properties. Today, the detection capability is assessed by a process of trial and error using dedicated test specimens. Thus, there is a vital need to develop a hybrid approach to predicting flaws detection ahead of time.

Then based on shearography models a methodology was implemented in a simulation capable of evaluating the engineering LST fringe pattern with a focus on vacuum excitation and circular delamination flaws.

This simulation was tested by comparing its results to representative cases from the literature and by conducting practical tests using the LST system. To carry out the practical experiment, a portable vacuum shearography system was used and dedicated test specimens were designed and created in the FBH configuration. The simulation results showed a good agreement with the literature representative cases and experiments results.

Subsequently, "Detection Capability Envelopes" were constructed for the LST method and making it possible to assess the detection capability of flaws depending on a variety of parameters. Investigation of the detection capability and construction of these envelopes was performed for the three most common types of structures in aviation – aluminum skin, composite solid laminate and composite sandwich structure. This, while analyzing the differences in detection capabilities between these structures.

The developed simulation as well as the detailed detection envelopes will make it possible to assess the LST detection capability in advance and will allow for a more correct design of the test specimens and to optimize the test parameters. These envelopes, as well as others that can be built based on the methodology and technique presented herein, can be used as a guide for all developers of test procedures using the LST method for effective and accurate detection of flaws in aviation structures – which will lead to improve the flight safety.

Contact Author Email Address

mailto:abramovich.haim@gmail.com or haim@technion.ac.il

Copyright Statement

The authors confirm that they, and/or their company or organization, hold copyright on all of the original material included in this paper. The authors also confirm that they have obtained permission, from the copyright holder of any third party material included in this paper, to publish it as part of their paper. The authors confirm that they give permission, or have obtained permission from the copyright holder of this paper, for the publication and distribution of this paper as part of the ICAS proceedings or as individual off-prints from the proceedings.

References

- 1. Baker, A., Dutton, S. and Kelly, D., *Composite materials for aircraft structures 2nd Ed*.AIAA, ISBN 978-1563475405, Chapter 1 pp. 1-21, 2004.
- Mrazova, M., Advanced composite materials of the future in aerospace industry, INCAS BULLETIN, Volume 5, Issue 3, pp. 139-150, 2013.
- Campbell, F. C., Structural composite materials, ASM international, ISBN 978-1-61503-037-8, Chapter 1, pp. 1-18, 2010.
- 4. Thori, P., Sharma, P. and Bhargava, M., An approach of composite materials in industrial machinery: advantages, disadvantages and applications, *International Journal of Research in Engineering and Technology*, Volume: 02 Issue: 12, eISSN: 2319-1163 | pISSN: 2321-7308, 6p., 2013.
- 5. Hale, J., Boeing 787 from the ground up, *Aeromagazine QTR406*, a quarterly publication boeing.com/commercial/aeromagazine, pp. 17-23, 2008.
- 6. Hiken, A., *The Evolution of the Composite Fuselage: A manufacturing perspective*. SAE International Journal of Aerospace, Intech open, 2018.
- 7. Xu, B., Li, H. Y., Advanced composite materials and manufacturing engineering, Trans Tech Publications, selected peer reviewed papers from the 2012 *International Conference on Advanced Composite Materials and Manufacturing Engineering (CMME2012)*, October 13-14, 2012.
- 8. Researchandmarkets.com, Aerospace composites materials market report: Trends, forecast and competitive analysis. ID: 4846250, 2019.
- 9. Liu, L., Zhang, B.-M., Wang, D.-F. and Wu, Z.-J., Effects of cure cycles on void content and mechanical properties of composite laminates, *Composite Structures* Vol. 73, No. 3, pp. 303–309, 2006.
- 10. Ghobadi, A., Common type of damages in composites and their inspections, *World Journal of Mechanics*, Vol.07 No.02, Article ID:74281, pp. 24-33, 2017.
- 11. Reifsnider, K. L., *Damage in composite materials*. ASTM SPECIAL TECHNICAL PUBLICATION 775, pp. 7-14, 1982.
- 12. Dhulkhed, S. and Narayanswamy, S., ANSYS simulation as a feasibility study for High repetition laser ultrasonic non-destructive evaluation (NDE), Photonics North (PN), Corpus ID: 1242182, 2016.
- 13. Elbaz, Y., Hybrid approach to predict and optimize flaw detection capabilities using laser shearography, Master Thesis at Faculty of Aerospace Engineering, Technion, I.I.T., 32000, Haifa, Israel, Feb. 2022, 153p.
- 14. Akbari, D., Soltani, N. and Farahani, M., Numerical and experimental investigation of defect detection in polymer materials by means of digital shearography with thermal loading, *Proceedings of the Institution of Mechanical Engineers, Part B: Journal of Engineering Manufacture* 227(3), pp. 430-442, 2013.
- 15. Sharpe, W. N. Jr, *Springer handbook of experimental solid mechanics*. ISBN: 978-0-387-26883-5, Part C 23.2, pp. 660-672, 2008.
- 16. Yang, L., Chen, F., Steincheng, W. and Hung, M.Y., Digital shearography for nondestructive testing: Potentials, limitations, and applications, *Journal of Holography and Speckle*, Volume 1, Number 2, pp. 69-79, 2004.
- 17. Hung, Y. Y., A speckle-shearing interferometer: A tool for measuring derivatives of surface displacements, *Optics Communications*, Volume 11, Issue 2, pp. 132-135, 1974.
- 18. Francis, D., Tatam, R. P. and Groves, R. M., Shearography technology and applications: a review, Measurement Science and Technology, Volume 21, Number 10, 2010.
- 19. Bossi, R.H., (Technical ed.), *Aerospace NDT, ASNT Industry Handbook*. ISBN: 978-1-57117-340-9, Chapter 12: "Shearographic and Holographic testing", John W. Newman, 2014.
- 20. LTI-laserndt.com
- 21. Timoshenko, S. P. and Woinowsky-Krieger, S., *Theory of plates and shells (2nd Ed.).* McGraw Hill, New York, ISBN: 0-07-064779-8, 1959.
- 22. Waldner, S. and Goudemand, N., Quantitative strain analysis with image shearing speckle pattern interferometry, in *Interferometry in speckle light: theory and applications*. P. Jacquot and J.-M. Fournier, eds., pp. 319–326, 2000.

- 23. Laser Technology, Inc. Holography and Shearography Level III-General interpretation and evaluation of test results, presentation, 2019.
- 24. Assignment 4: ESPI/Digital Holography And Digital Shearography, https://www.chegg.com/homework-help/questions-and-answers/assignment-4-espi-digital-holography-digital-shearography-fig-1-2-show-holographic-shearog-q27826442.
- 25. Yang, F., Ye, X., Qiu, Z., Zhang, B., Zhong, P., Liang, Z.Y., Sun, Z. and Zhu, S., The effect of loading methods and parameters on defect detection in digital shearography, *Results in Physics*, Volume 7, pp. 3744-3755, 2017.